Journal of The Electrochemical Society, **147** (8) 3100-3105 (2000)
S0013-4651(99)12-095-0 CCC: $7.00

Spectroscopic Investigations of Borosilicate Glass and Its Application as a Dopant Source for Shallow Junctions

M. Nolan,[a] T. S. Perova,[a,z] R. A. Moore,[a] C. E. Beitia,[b] J. F. M[c]Gilp,[b] and H. S. Gamble[c,*]

[a]*Department of Electronic and Electrical Engineering,* [b]*Department of Physics, University of Dublin, Trinity College, Dublin 2, Ireland*
[c]*Department of Electronic Engineering, The Queen's University of Belfast, Belfast, Northern Ireland*

Borosilicate glass was investigated as a dopant source for proximity rapid thermal diffusion. A borosilicate gel was spun onto a silicon wafer and the layer was rapid thermally processed to convert it to a borosilicate glass. Fourier transform infrared spectroscopy, spectroscopic ellipsometry, and sheet resistance measurements were used to understand and subsequently optimise the conversion of the gel to a borosilicate glass. The optimum conversion step, which avoided any boron loss from the borosilicate glass layer, was a curing step of 900°C for 45 s. Secondary ion mass spectrometry was used to measure the boron dopant profile of a silicon wafer that was doped with the borosilicate glass layer. The wafer had a surface dopant concentration of 4.7×10^{19} cm^{-3} and a junction depth of 65.5 nm. Junction diodes, which were fabricated using the glass layer as a dopant source, displayed excellent characteristics, with very low leakage currents and a near ideal forward slope.

Manuscript submitted December 12, 1999; revised manuscript received April 27, 2000.

The integrated circuit industry's continuous drive toward smaller and faster devices for the next generation of ultralarge-scale integrated (ULSI) circuitry puts critical demands on vertical scaling. Source/drain junctions with depths <70 nm in 0.18 μm technology[1] are required in metal oxide semiconductor field-effect transistors (MOSFETs) to reduce short channel effects. The greatest challenge arises in the fabrication of boron doped p^+-n junctions. At present, ULSI and very large-scale integrated (VLSI) silicon technologies depend primarily on ion implantation for doping. However, there are limitations on this technique in the formation of shallow boron junctions.[2-4] Ion implantation generates defects in silicon, and these defects must be annealed out at high temperatures after the implant. The high diffusivity of boron in silicon[5] and transient-enhanced diffusion of channeling tails during the thermal anneal, makes control of shallow junction depths difficult.

In this paper, proximity rapid thermal diffusion (RTD) is used as a technique for fabricating shallow boron junctions.[6] A spin-on dopant (SOD) deposited onto a silicon wafer was used as a planar dopant source during RTD. The wafer configuration during proximity RTD is shown in Fig. 1. This technique is very suitable for shallow junction formation for several reasons: (*i*) the dopant source is quick and easy to prepare, (*ii*) there are no defects introduced into the wafers during the diffusion process, and (*iii*) the dopant diffusion is minimized since the wafers are heated to high temperatures for short times.

The SOD is in the form of a borosilicate gel, and is commercially available from Filmtronics, USA. On heating, the composition and structure of the SOD gel changes to that of a borosilicate glass (BSG). The boron supply from the dopant source changes as the structure of the SOD gel changes.[7] Therefore, in order to use one dopant source to dope several wafers repeatably, it is important that the borosilicate gel is initially converted into a stable BSG dopant source. Fourier transform infrared (FTIR) spectroscopy and spectroscopic ellipsometry are used to determine, and subsequently optimise, the conversion of the gel to BSG.

In the past decade, a number of investigations have been performed to understand how different thermal treatments influence the properties of SOD and spin-on glass (SOG) films. Information on different properties, such as doping efficiency, density, refractive index, and thickness have been found for phosphosilicate glass (PSG) films in Ref. 8-12 and for SOG films in Ref. 13-15. However, very few studies have been done on spin-on dopant BSG films.[16-19] Detailed investigations were performed on BSG[20-25] and borophosphosilicate (BPSG)[26-34] films, obtained by low pressure and atmospheric pressure chemical vapor deposition (LPCVD and APCVD). However, as was noted by Becker *et al.*,[28] the properties of these films strongly depends on the preparation technique. This paper presents the detailed FTIR and ellipsometric analysis of BSG films spin-coated on silicon wafers. As deposited, the SOD layer had a thickness of 120 nm. This layer is very thin in comparison to the BSG layers that were used in previous works. It should also be noted that there is no thin capping silicon dioxide layer on the surface of the BSG films studied here, since the concentration of boron is not high and the films do not absorb moisture on exposure to the atmosphere after the curing process. The measurements were repeated six months after the initial measurements were made, and there were no changes in the FTIR spectra recorded.

Experimental

Proximity rapid thermal diffusion.—Czochralski grown 4 in. n-type, <100> oriented, 9-15 Ω cm resistivity silicon wafers were

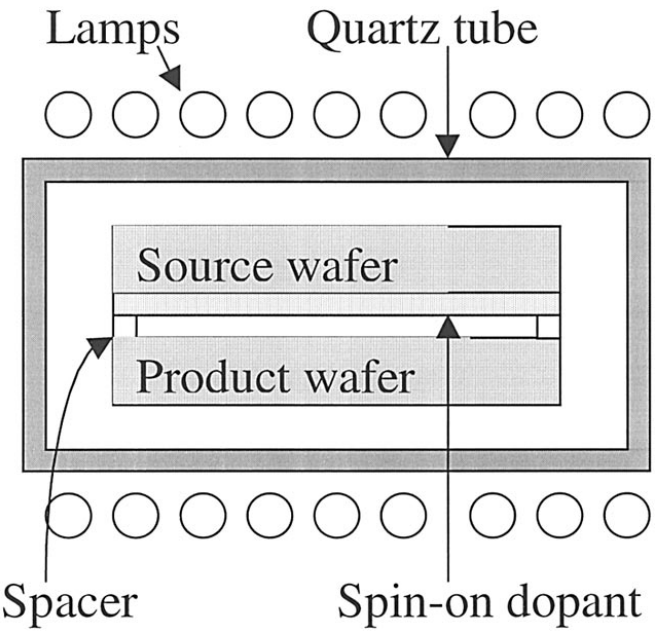

Figure 1. Wafer configuration during proximity RTD.

* Electrochemical Society Active Member.
z E-mail: perovat@tcd.ie

S0013-4651(99)12-095-0 CCC: $7.00

used throughout this study. As-received wafers were cleaned using H_2SO_4:H_2O_2 followed by a HF dip. SOD gel was spun onto the wafers at 6000 rpm for 15 s. The SOD contains ethanol as a solvent. Therefore, following application of the SOD, it was necessary to bake the wafers at 200°C to evaporate moisture and light organics from the dopant layer.[6,7] The rapid evaporation of the solvent during film deposition (through the spinning) leads to the formation of a porous gel film. The film structure in this case[13] strongly depends on the molecular weight distribution of the oligomers present in the solution. Thus, even after baking at 200°C, silanol (Si-OH), molecular water, and ethanol remain in the gel network to some extent. Fully dense films are only produced after heat-treatment at temperatures between 800 and 1200°C.[13,32]

Dopant source wafers were cured in a Sitesa rapid thermal processor (RTP) at different temperatures in the range 800-1000°C for 2-60 s (Table I), to convert the SOD gel to a BSG layer prior to RTD. FTIR and spectroscopic ellipsometry were used to determine, and subsequently optimize, the conversion of the gel to a BSG layer.

Following the stabilization of the dopant source, the source wafer was then stacked in proximity to a silicon product wafer on 0.5 mm silicon spacers, Fig. 1. Several silicon product wafers were doped using the optimised dopant source. All rapid thermal heat treatments were performed in 25% O_2:75% N_2.

FTIR Measurements.—The measurements on BSG films were performed in the spectral range from 4500 to 500 cm^{-1} with a Fourier transform Bio-Rad FTS60A spectrometer using a Globar source, a KBr beam splitter, and a mercury cadmium telluride (MCT) detector. The spectra were collected with 8 cm^{-1} resolution, and 64 scans were averaged for each spectrum to improve the signal-to-noise ratio. A bare silicon substrate was used as a reference for all of the samples, and the analysis of the transmission spectra was performed while neglecting reflectance. A clear and detailed analysis of the different films requires consideration of spectra both in the high frequency region (from 3000 to 2000 cm^{-1}) and in the low frequency region (from 1600 to 400 cm^{-1}). The spectra are the superposition of the spectra of the BSG and the silicon wafer and it is necessary to subtract the spectrum of the bare wafer from the measured spectra in order to obtain the spectra for the BSG. Hence, all spectra discussed below are difference spectra. It should be noted that the influence of the substrate absorption becomes especially important if heat-treated samples are analyzed, as was shown by Becker *et al.*[28] However, we believe that, due to the extremely short thermal treatment in the RTP reactor (the maximum time used was 60 s), there is no change to the substrate absorption.

Table I. Rapid thermal treatment to convert SOD gel to BSG.

Sample	Curing temperature (°C)	Curing time (s)
1	800	10
2	800	25
3	800	45
4	800	60
5	850	10
6	850	25
7	850	45
8	850	60
9	900	10
10	900	25
11	900	45
12	900	60
13	950	5
14	950	10
15	950	25
16	950	45
17	1000	2
18	1000	5
19	1000	25
21	1000	45

Spectroscopic ellipsometry measurements.—The refractive index and the thickness of the sample were obtained by means of spectroscopic ellipsometric measurements. This technique has been widely used for the characterization and study of the physical properties of thin films.[35-37]

The samples were measured at room temperature with a rotating polarizer spectroscopic ellipsometer (SOPRA GESP5) in the visible to near ultraviolet wavelength range (225–880 nm). For each spectrum, 250 points were measured, giving a wavelength resolution of 3 nm. The data were collected using the current tracking mode for the position of the analyzer in order to improve the accuracy of the measurements. In order to improve the accuracy in determining the physical parameters of the samples, each spectrum was measured at two different angles of incidence (65 and 75°). Several different models were used to fit the data measured ($\tan \Psi$ and $\cos \Delta$) simultaneously at the two angles of incidence. A suitable three-layer model (air, oxide layer, silicon), using a Cauchy law fit for the oxide layer, was chosen based on the accuracy of the results obtained (a detailed description of this model will be presented in a separate paper). This paper presents the results obtained from this model and compares them to results obtained from FTIR.

Secondary ion mass spectrometry (SIMS) and sheet resistance measurements.—The sheet resistance of the wafers was measured using a Jandel four-point probe. The boron concentration profiles of the product wafers were measured using a CAMECA IMS 3F secondary ion microscope in the National Microelectronics Research Centre (NMRC), Ireland.

Device fabrication and characterization.—Having optimized the conversion of the borosilicate gel to a BSG, diodes were fabricated using BSG as a dopant source in proximity RTD. A four-mask process was used to produce p^+-n diodes. The substrate was wet oxidized at 1000°C to produce a masking oxide layer of thickness approximately 0.4 μm. This oxide was patterned and a p-type diffusion from a boron nitride disk was carried out at 1000°C for 20 min, followed by a 60 min drive-in at 1000°C, to form deep p-type junctions. A second mask was used to open the windows for the very shallow proximity RTD p-type regions. An LPCVD oxide was deposited from a tetraethoxyorthosilane (TEOS) source at 720°C. Opening contact windows in this oxide layer, followed by aluminum metallization, completed manufacturing of the device. Finally, the forward and reverse current-voltage (I-V) characteristics of the p^+-n diodes were measured.

Results and Discussion

FTIR.—IR spectroscopy is known to be a fast and nondestructive method of determining a number of important properties of dielectric films. Those properties are boron and phosphorous concentration, absorbed water content, chemical bonds structure, thickness, and density.[20-22,40] The ratio of the B–O band peak intensity at a frequency near 1370 cm^{-1} to the Si-O-Si absorbance maximum near 1075 cm^{-1} is widely used to determine the boron content for glass films of thickness up to 2.5 μm.[20-25]

FTIR was used to investigate the structure and properties of the SOD layer after the rapid thermal curing (RTC) process step. The wafers were cured at 800, 850, 900, 950, and 1000°C for 2–60 s, Table I. The FTIR spectra for the wafers treated at 900 and 1000°C are shown in Fig. 2 and 3. These spectra clearly show the change in structure with variation in temperature and time. In particular, as the heating time is increased, the Si-O-Si asymmetric stretching vibration (AS) band at ~1075 cm^{-1} shifts to a higher frequency and the absorption intensity increases. This shows that the silicon dioxide thickness has increased and the SOD layer has densified.[15,20-22]

For a given temperature, the B-O stretching vibration band in the region 1370-1440 cm^{-1} shifts to a lower frequency as the heating time increases (Fig. 2 and 3). This is a characteristic change, which occurs on densification of borosilicate glass.[20,21] The absorption intensity and the contour of this band also changes significantly as the heating time is increased. These changes were observed for all of the (RTC) temperatures investigated. The intensity of the broad band

S0013-4651(99)12-095-0 CCC: $7.00

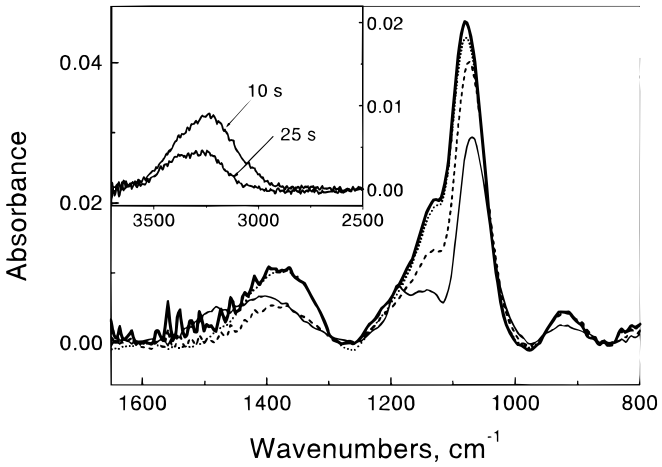

Figure 2. IR absorbance spectra of SOD layers that were annealed at 900°C for various times: 10 s (thin solid line), 25 s (dashed line), 45 s (dotted line), 60 s (heavy solid line).

that appears at ~1430 cm^{-1} (peak position of B–O stretching vibrations[20-22]) decreases rapidly with time and the peak shifts to a lower frequency. Then the intensity of this band increases again and reaches a saturation value with a peak position at ~1370 cm^{-1}. This complicated behavior can be explained by the influence of a number of different processes: (*i*) the decrease in film thickness as a result of the layer shrinking with temperature, (*ii*) the evaporation of the organic residuals from boron and silicate oligomers, and (*iii*) the formation of the borosilicate network through the bridging oxygen atoms.

The existence of organic residuals (attached to the Si and B atoms[38-40]) after baking at 200°C and even after very short RTC treatment can be verified by the observation of the vibrational bands belonging to hydroxyl and ethoxy groups, in the high frequency region (2400–3600 cm^{-1}) and at frequencies 1200 cm^{-1} (OH) and at 1635 cm^{-1} (CH_3).[6,7,22,32,41] The dramatic decrease in the absorption intensity of the OH stretching vibration band (shown as insets in Fig. 2 and 3) verifies that the progressive loss of the OH groups in the form of H_2O and C_2H_5OH due to the chemical reactions described in Ref. 38, 40. This result indicates that during thermal treatment, the hydrolysis and condensation reactions are continuing, releasing water and ethanol, and producing to Si–O–Si, B–O–B, and Si–O–B bonds[34,38-40] at the expense of the Si–OH, B–OH, Si–OR, and B–OR groups. This is also consistent with the growth of the Si–O–Si and Si–O–B vibrational bands at 1075 and 910 cm^{-1}, respectively, with increasing temperatures. The rate of loss depends on the RTC process temperature. Enhancement of band intensity with temperature is explained by incorporation of the B–OH groups[38,39] into the borosilicate phase, during which Si–O–B bonds are progressively formed. The observed minimum in the intensity of B–O band at certain temperatures and times occurs during the transformation of tetraborate to borate and then to a borosilicate glass. At the intermediate stage, some boron may exist in ionic forms that are not IR active. The minimum observed for B–O peak intensity may be explained by the presence of IR inactive intermediate products that are formed during reconstruction of the layer rather than by boron loss from the layer (Fig. 2 and 3). However, the shift of the B–O band at ~1370 cm^{-1} to the high-frequency side seen in Fig. 3 after 45 s treatment at 1000°C is due to the boron diffusion into the underlying silicon.

The band at 910 cm^{-1} can also be used to determine when the BSG forms. This band belongs to the bending vibration of B–O–Si units, and is a characteristic band, which appears on the formation of BSG.[20-22] The band intensity increases as the RTC time increases (Fig. 2, 3). Figure 3, in particular, shows the increase in intensity and a stabilization of the peak at 25 s.

Analysis of the ratio of two vibrational bands B–O/Si–O (B–O at 1370 cm^{-1} and Si–O–Si at 1075 cm^{-1}) allows the concentration of the boron in the dopant layer to be determined.[20-25] Figure 4 shows the dependence of the B–O/Si–O ratio on RTC time. For 800°C, there is a very little small change in the ratio between 25 and 45 s, which signifies a very slow rate of conversion of the gel to a glass. For 900°C, the ratio reaches a maximum value of 0.2 after 45 s cure and remains the same after a 60 s cure. The 1000°C profile reaches a maximum at a shorter time of 25 s.

Spectroscopic ellipsometry.—The refractive index and the thickness of the SOD layers have been determined from spectroscopic ellipsometry measurements. Figure 5 shows the refractive index values as a function of the curing time for different temperatures. All of the samples have a high value of refractive index for short curing times, ≤10 s. These high initial values are due to light organic residuals in the SOD layer, the existence of which are clearly shown in Fig. 2 and 3 by the presence of the 3000-3500 cm^{-1} band.

There is a significant decrease in refractive indices for curing times >10 s, following the evaporation loss of the organic residuals. A similar behavior was observed for SOG films due to the loss of hydroxyl and ethoxy groups.[14] It is known that the presence of such molecular functional groups in BSG increases the refractive index, and that the loss of these groups reduces the refractive index.[14,42] This observation is also consistent with the FTIR results (Fig. 2 and 3), which show a reduction in the OH band intensity in the 3000-3500 cm^{-1} region as hydroxyl groups are lost. The refractive indices decrease to values between 1.47 and 1.55, which are typical values for BSG.[42]

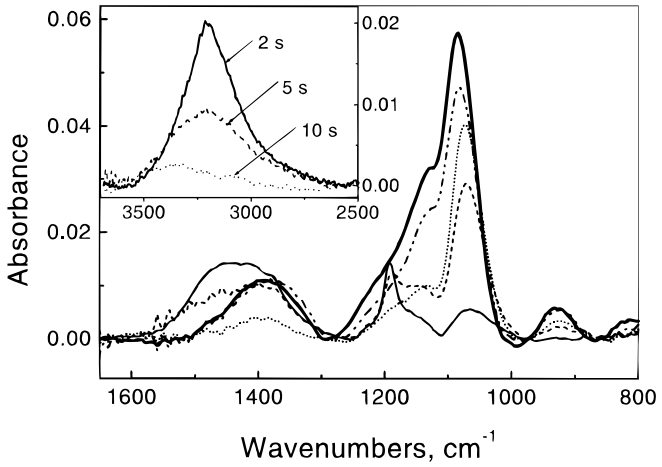

Figure 3. IR absorbance spectra of SOD layers that were annealed at 1000°C for various times: 2 s (thin solid line), 5 s (dashed line), 10 s (dotted line), 25 s (dashed-dotted line), 60 s (heavy solid line).

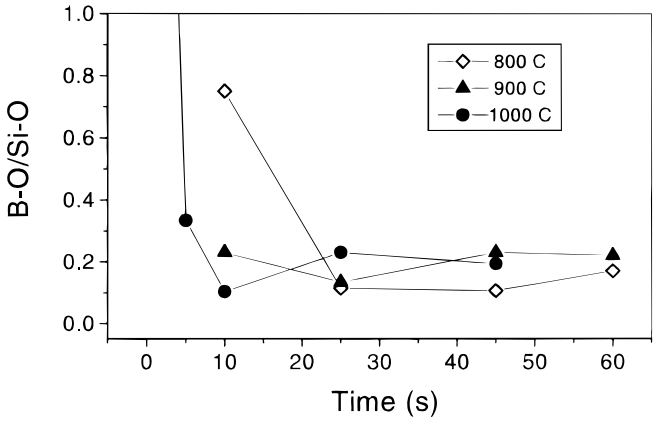

Figure 4. The dependence of the B–O/Si–O infrared peak ratio on curing time for different temperatures.

S0013-4651(99)12-095-0 CCC: $7.00 © The Electrochemical Society, Inc.

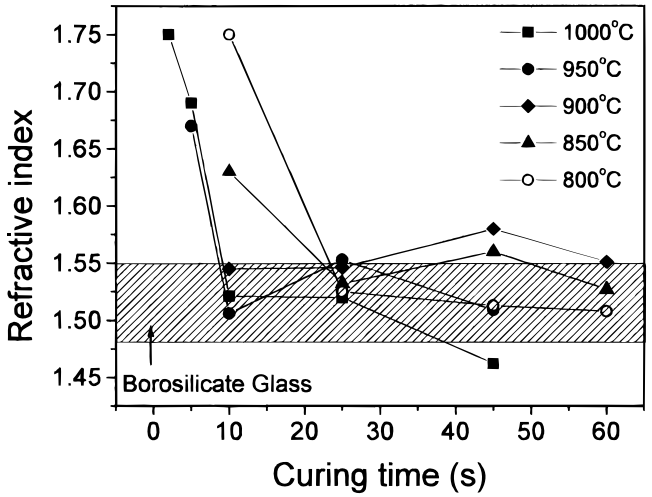

Figure 5. The dependence of the refractive index of SOD layers on RTA temperature and time.

Initially, an increase in the refractive index could be expected due to the densification of the gel to a BSG structure.[14] However, the decrease caused by the evaporation of the organic residuals (0.25-0.15) is one order of magnitude bigger than the expected decrease on BSG densification (0.025).[14,15]

Oxide growth at the underlying Si/BSG interface might also be expected because the thermal processing is taking place under an oxygen-containing atmosphere. Sol-gel layers can retain a structure of interconnected pores, even after high temperature thermal treatment. We have estimated the porosity of the BSG layer to be about 3%.[43] Hence, the growth of SiO_2 beneath the BSG layer, via the interconnected pores of the layer, should also be considered. However, it is very difficult to observe changes in the global refractive index due to any densification or oxidation process while the organic residuals influence the results.

For curing times >10 s, the refractive index continues to vary with temperature and time. There are several factors that must be taken into consideration: (*i*) the refractive index will decrease if the underlying Si oxidizes, because of the decrease in the overall B_2O_3/SiO_2 ratio, (*ii*) the refractive index will increase as the layer becomes more dense, and (*iii*) any diffusion of boron from the BSG layer will also cause a decrease in the refractive index.

At 800°C, there is no significant change in refractive index for curing times >20 s. This is in good agreement with the B–O/Si–O dependence at 800°C measured by FTIR and further verifies that any change is very slow at this temperature. The refractive index for 850 and 900°C increases by a small amount and reaches a maximum value at 45 s. This refractive index behavior is consistent with densification of the BSG layer, evidence for which also comes from the characteristic decrease in B–O frequency (1400 cm^{-1} region in Fig. 2 and 3). Next, the refractive index for the 850°C and 900°C samples decreases by 0.03 between the 45 and 60 s cures. Oxidation of the underlying Si or boron out-diffusion from the BSG layer would produce such a decrease. The film thickness determined from the spectroscopic ellipsometry calculations (Fig. 6), is in excellent agreement with the Si–O FTIR peak intensity, and shows that the film thickness increases with curing time. In contrast, there was no difference in the sheet resistance of the silicon source wafer before and after the 850 and 900°C RTC steps, confirming that the boron did not diffuse into the silicon source wafers, in significant quantities, at these process temperatures. The decrease of 0.03 in refractive index must arise from the oxidation of the underlying silicon. The oxidation rate is a little higher than that of a normal rapid thermal oxidation process. This is reasonable, as these layers are significantly thinner than normal thermal oxide layers.

At 950°C, the refractive index shows the same trend as the 850 and 900°C plots, except that the changes occur more rapidly. The increase in reaction rate at higher temperatures is evident in Fig. 6 by the more rapid increase in layer thickness. The measured refractive index value at 950°C is highest after a 25 s cure. This value is not as high as the maximum value measured for 900°C. However, the rapid rate of change occurring at 950°C means that the true maximum may not have been measured. After processing for 45 s, the refractive index decreases by over 0.03 from the 25 s value. In this case, however, both oxide layer growth and boron out-diffusion may be contributing to the decrease. In Fig. 3, the maximum B–O frequency position for 1000°C increases from 1370 to 1390 cm^{-1} between the 25 and 45 s cures. This change in frequency is consistent with a decrease of boron content in the BSG layer. Sheet resistance measurements also confirm that boron diffuses from the oxide layer into the underlying silicon. These trends are more pronounced for RTC at 1000°C but, due to the increase in the conversion rate at high temperatures, additional data points would be required to determine the detailed refractive index behavior.

The most favorable RTC process step would be at a temperature that does not result in boron loss from the BSG layer, since the layer is used as a boron dopant source, but that also converts the SOD gel to BSG in the shortest time possible. It is possible to determine the optimum conditions by combining the FTIR, spectroscopic ellipsometry, and sheet resistance results. We know from sheet resistance measurements, and from spectroscopic investigations, that boron diffuses from the BSG layer at temperatures greater than 900°C. As the rate of conversion increases with RTC temperature, a 900°C curing step will be more time efficient than thermal treatments at 800 or 850°C. Figures 4 and 5 shows that the BSG layer is in its most stable condition after a 45 s cure at 900°C. These are the optimum RTC conditions for the conversion of SOD gel to BSG.

The suitability of the converted BSG layer as a dopant source was determined by, first, doping a bare silicon wafer, and, second, by using the technique as a process step in the fabrication of a p^+-n diode. The SOD gel was heated to 900°C for 45 s and then stacked in proximity to a silicon wafer and heated to 1050°C for 5 s. Figure 7 shows the SIMS concentration depth profile of the product wafer. The wafer has a surface concentration of 4.7×10^{19} cm^{-3}; the concentration is 10^{18} cm^{-3} at a depth of 65.5 nm. Three wafers were doped with a single BSG layer, and sheet resistance measurements confirm that all of the wafers were equally doped, with a sheet resistance of approximately 530 Ω/m^2. For comparison, one product wafer was doped with a SOD gel that had not been converted to BSG. The boron concentration profile is also shown in Fig. 7. The wafer has a higher surface concentration and a deeper junction depth than the wafer that was doped with the BSG layer. Sheet resistance measurements show that the boron profile of wafers that were subsequently doped with this SOD gel continually change until the SOD gel has converted into

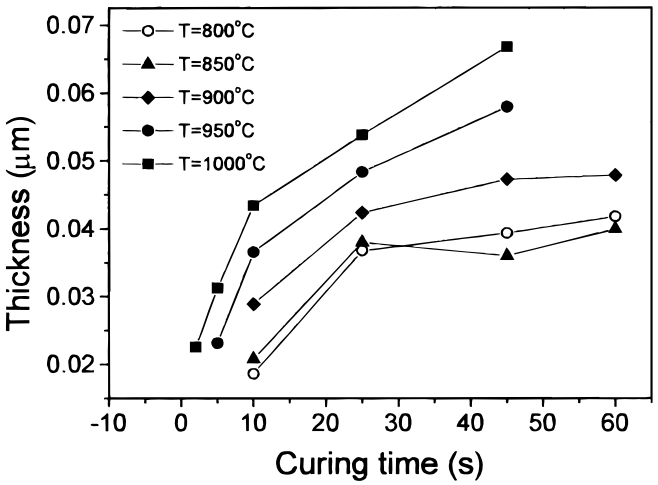

Figure 6. Variation in thickness of SOD layers, obtained from the spectroscopic ellipsometry measurements, with changing RTC temperature and time.

S0013-4651(99)12-095-0 CCC: $7.00

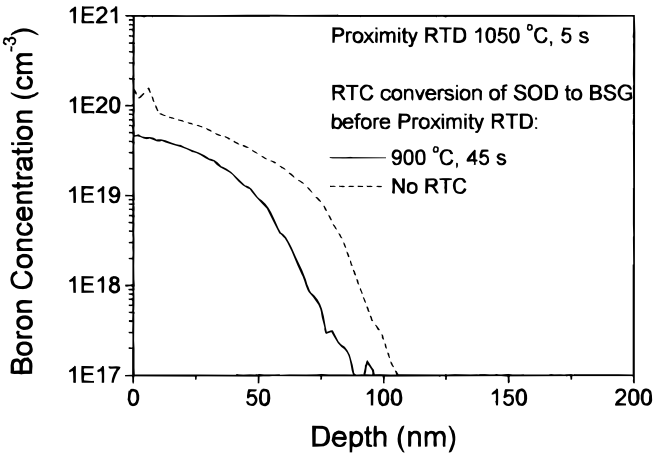

Figure 7. SIMS profiles of junctions that were formed by diffusion of boron from uncured and cured SOD.

a stable BSG dopant source. These results highlight the need to convert the borosilicate gel to a stable BSG layer.

Diodes were fabricated using proximity RTD to form shallow boron-doped junctions. Figure 8 shows the I-V characteristics for the diode. The forward bias turn-on voltage was 0.6 V, and the measured ideality factor was 1.07 over a 350 mV range. Under reverse bias, the diode has a sharp avalanche breakdown at −29 V. The leakage current observed is very low, rising to 50 pA as the diode approaches breakdown. A more detailed description of these devices are presented in a later paper.

Conclusions

The thermal conversion of a SOD borosilicate gel layer to a stable BSG dopant source layer has been achieved by combining the results of FTIR, spectroscopic ellipsometry, and sheet resistance measurments. The layers were cured in an RTP in the temperature range 800-1000°C for 2-60 s in an atmosphere of 25% O_2:75% N_2. The changes in the properties of the layer can be summarized as follows

1. The thickness of the layer increases with increasing temperature and time. This increase in thickness is attributed to oxide growth at the Si-BSG interface during the heat-treatment in an oxidizing ambient.

2. Initially, the refractive index decreases following the loss of organic residuals from the layer. The refractive index then increases as the BSG layer densifies, and subsequently decreases again as the underlying silicon oxidizes. For the 950°C and 1000°C treatments, the refractive index may decrease again due to boron diffusion from the BSG layer.

Heating at 900°C for 45 s was the optimum RTC process step required to convert the gel to a BSG, since there was no detectable boron loss from the BSG dopant source at this temperature. Very shallow junctions, with profiles suitable for MOSFET technology, were fabricated by RTD of boron from the stabilized BSG layer. Diodes were successfully manufactured, and displayed excellent electrical characteristics. From the forward I-V characteristics a value of 1.07 for the ideality factor was deduced and the reverse characteristic had a very low leakage current with a sharp breakdown at −29 V.

Acknowledgments

Intel Ireland is gratefully acknowledged for financial contributions toward this research project. The authors would also like to thank Professor J. K. Vij for use of his FTIR spectrometer..

References

1. *The National Technology Roadmap for Semiconductors*, p. 74, Semiconductor Industry Association, San Jose, CA (1997).
2. W. Eichhammer, M. Hage-Ali, R. Stuck, and P. Siffert, *Appl. Phys. A*, **50**, 405 (1990).
3. C. Park, K. M. Klein, Al. F. Tasch, R. B. Simonton, and G. E. Lux, *Tech. Dig. Int. Electron. Devices Meet.*, **67** (1991).
4. S. Hong, G. A. Ruggles, J. J. Wortman, and M. C. Ozturk, *IEEE Trans. Electron. Devices*, **38**, 476 (1991).

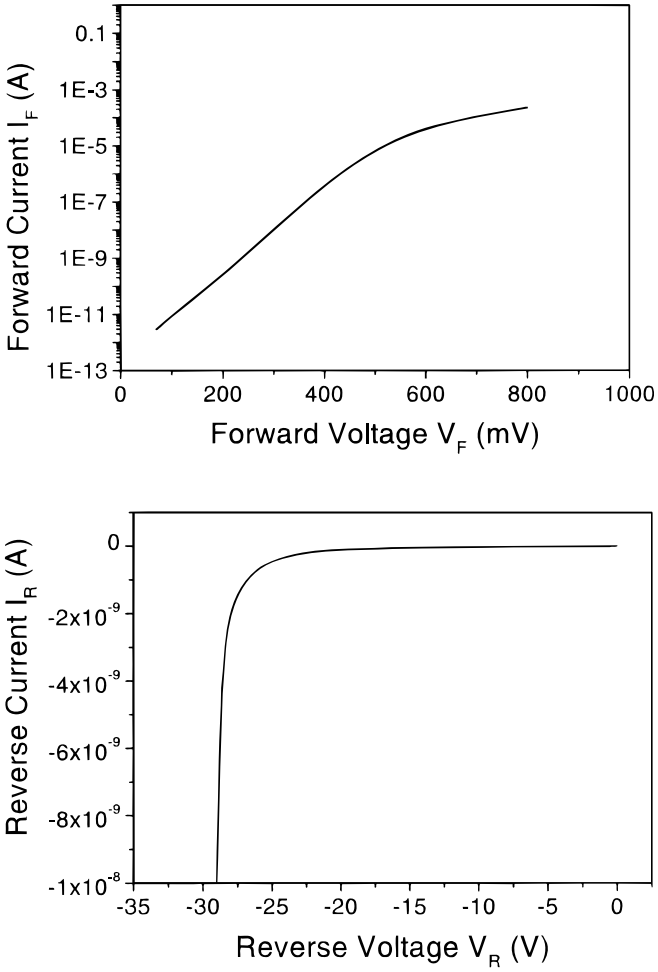

Figure 8. I-V characteristics of a p^+-n diode: (a) forward bias characteristics (b) reverse bias characteristics.

5. R. B. Fair, *Proc. IEEE*, **79**, 1687 (1990).
6. W. Zagozdzon-Wosik, J. C. Wolfe, and C. W. Teng, *IEEE Electron. Devices Lett.*, **12**, 264 (1991).
7. M. Nolan, T. Perova, R. A. Moore, and H. S. Gamble, *J. Non-Cryst. Solids*, **254**, 89 (1999).
8. W. Zagozdzon-Wosik, P. Grabiec, F. Romero-Borja, L. T. Wood, and G. Lux, *Mater. Res. Soc. Symp. Proc.*, **303**, 297 (1993).
9. S. Montandon, N. Zagozdon-Wosik, J. Li, W. T. Taferner, and B. Bensaoula, in *Cleaning Technology in Semiconductor Device Manufacturing IV*, R. E. Novak and J. Ruzyllo, Editors, PV 95-20, p. 552, The Electrochemical Society Proceedings Series, Pennington, NJ (1955).
10. W. Zagozdzon-Wosik, P. Grabiec, and G. Lux, *J. Appl. Phys.*, **75**, 337 (1994).
11. W. Zagozdzon-Wosik, P. Grabiec, and G. Lux, *IEEE Trans. Electron Devices*, **41**, 2281 (1994).
12. P. Grabiec, W. Zagozdzon-Wosik, and G. Lux, *J. Appl. Phys.*, **78**, 204 (1995).
13. R. M. Almeida and C. G. Pantano, *J. Appl. Phys.*, **68**, 4225 (1990).
14. L. Ventura, B. Hartiti, A. Slaoui. J.-C. Muller, and P. Siffert, *Mater. Res. Soc. Symp. Proc.*, **284**, 197 (1993).
15. A. Slaoui, L. Ventura, A. Lachig, R. Monna, and J. C. Muller, *Mater. Res. Soc. Symp. Proc.*, **387**, 365 (1995).
16. D. M. Haaland and C. J. Brinker, *Mater. Res. Soc. Symp. Proc.*, **32**, 267 (1984).
17. M. Rastogi, W. Zagozdzon-Wosik, F. Romero-Borja, J. M. Haddleson, R. Beavers, P. Grabliec, and L. T. Wood, *Mater. Res. Soc. Symp. Proc.*, **342**, 369 (1994).
18. S. Mone, W. Zagozdzon-Wosik, and M. Rastogi, *Mater. Res. Soc. Symp. Proc.*, **405**, 351 (1996).
19. D. J. Taylor, D. Z. Dent, D. N. Braski, and B. D. Fabes, *J. Mater. Res.*, **11**, 1870 (1996).
20. W. Kern, *RCA Rev.*, **32**, 429 (1971).
21. J. Wong, *J. Electron. Mater.*, **5**, 113 (1976).
22. W. A. Pliskin, in *Semiconductor Silicon/1973*, H. R. Huff and R. R. Burgess, Editors, p. 506, The Electrochemical Society Proceedings Series, Princeton, NJ (1973).
23. A. S. Tenney, *J. Electrochem. Soc.*, **118**, 1658 (1971).
24. E. A. Taft, *J. Electrochem. Soc.*, **118**, 1985 (1971).
25. A. S. Tenney and J. Wong, *J. Chem. Phys.*, **56**, 5516 (1972).
26. W. Kern and G. L. Schnabe, *RCA Rev.*, **43**, 423 (1982).

S0013-4651(99)12-095-0 CCC: $7.00

27. W. Kern, W. A. Kurylo, and C. J. Tino, *RCA Rev.*, **46**, 117 (1985).
28. F. S. Becker, D. Pawlik, H. Shäfer, and G. Staudigl, *J. Vac. Sci. Technol*, **B4**, 732 (1986).
29. J. E. Franke, T. M. Niemczyk, and D. Haaland, *Spectrochim. Acta*, **50A**, 1687 (1994).
30. R. A. Carpio and J. Taylor, *Proc. SPIE-Int. Soc. Opt. Eng.*, **2638**, 38 (1995).
31. T. W. Dyer, *J. Electrochem. Soc.*, **145**, 3950 (1998).
32. S. Rojas, R. Comarasca, L. Zanotti, A. Borghesi, S. Sassella, G. Ottaviani, L. Moro, and P. Lazzeri, *J. Vac. Sci. Technol.*, **B10**, 633 (1992).
33. L. D. Madsen, A. C. de Wilton, and J. S. Mercier, *Chemtronics*, **5**, 35 (1991).
34. D. M. Haaland and C. J. Brinker, *Mater. Res. Soc. Symp. Proc.*, **32**, 267 (1984).
35. I. Susuki, M. Ejima, K. Watanabe, Y. Xiong, and T. Saitoh, *Thin Solid Films*, **313-314**, 214 (1998).
36. B. Drevillon, *Thin Solid Films*, **313-314**, 625 (1998).
37. S. Bruynooghe, F. Bertin, A. Chabli, J.-C. Blanchard, and M. Couchaud, *Thin Solid Films*, **313-314**, 722 (1998).
38. M. Nogami and Y. Moriay, *J. Non-Cryst. Solids*, **48**, 359 (1982).
39. A. D. Irwin, J. S. Holmgren, T. W. Zerda, and J. Jonas, *J. Non-Cryst. Solids*, **89**, 191 (1987).
40. M. A. Villegas, J. M. Fernández Navarro, *J. Mater. Sci.*, **23**, 2464 (1988).
41. R. M. Levin, *J. Electrochem. Soc.*, **129**, 1765 (1982).
42. T. S. Izumitani, *Optical Glasses*, p. 17, American Institute of Physics, New York (1986).
43. M. Nolan, T. S. Perova, R. A. Moore, C. E. Beitia, J. F. McGilp, and H. S. Gamble, In preparation.